

Simultaneous Single-Particle Tracking and Visualization of Domain Structure on Lipid Monolayers

Martin B. Forstner,^{*,†,‡} Douglas S. Martin,^{†,‡} Ann M. Navar,[†] and Josef A. Käs^{†,‡}

Center for Nonlinear Dynamics, Department of Physics, University of Texas at Austin, Austin, Texas 78712, and Physics Department, University of Leipzig, D-04103 Leipzig, Germany

Received January 29, 2003. In Final Form: April 4, 2003

A new method is presented that combines dual fluorescence microscopy and single-particle tracking (SPT) to investigate the impact of spatial inhomogeneities in membranes on lateral diffusion within Langmuir monolayers. In contrast to previous SPT experiments, random walks of individual fluorescent tracer particles and the structure of the membrane are simultaneously imaged. Monolayers of 1,2-dimyristoyl-*sn*-glycero-2-phosphoethanolamine (DMPE) in the liquid condensed/liquid expanded phase are used to model the inhomogeneous plasma membrane, while the fluorescent particles embedded in the membrane serve as model proteins. The interactions between tracers and the domain boundary and the resulting change in their random walks are directly observed. Since this technique permits systematic SPT studies of diffusion in inhomogeneous monolayers, its extensions to more biologically relevant monolayers are laid out as well.

Introduction

Although transport processes in disordered media¹ are the focus of ongoing basic research² in physics and material science, many fundamental questions remain unanswered. For example, the impact of geometric disorder in porous materials on thermodynamic transport properties, such as diffusion, is not yet understood. In addition, because of the importance of such processes within inhomogeneous living matter, these same questions have also recently gained attention within biological research.³

It is long known that essential cellular functions, like intercellular signaling, rely on transport processes within the plasma membrane.⁴ In the signaling process, information is transmitted over large distances throughout the cell by means of a highly connected network of chemical reactions which exchange their reactants and products. For example, the messenger molecule PIP₂ has to diffuse laterally in the membrane in this signal transduction cascade.⁵

It took the recent advent of new investigative tools such as optical traps,⁶ single-molecule imaging,⁷ fluorescence correlation spectroscopy,⁸ and single-particle tracking (SPT)⁹ to recognize that the plasma membrane is not the simple "fluid mosaic" of Singer and Nicolson.¹⁰ Instead, the many different membrane structures found and

characterized^{11,12} show that the plasma membrane is a complex inhomogeneous two-dimensional fluid with structures over many time and length scales.¹³

To elucidate the intricate relationship between the membrane structure and control of information transmission, it is important to understand the effects of an inhomogeneous environment on two-dimensional diffusion. To that end, we have developed a technique to study the random motion of individual fluorescent beads in heterogeneous model membranes, where both individual particle motion and membrane structure are imaged simultaneously. This is achieved by adding dual fluorescence capabilities to our previously described method¹⁴ for SPT in monolayers at the air/water interface. We demonstrate this dual-image technique in our experiments with NeutrAvidin-coated, yellow-green fluorescent beads incorporated in a Texas Red–DPPE (Texas Red 1,2-dipalmitoyl-*sn*-glycero-3-phosphoethanolamine) doped 1,2-dimyristoyl-*sn*-glycero-2-phosphoethanolamine (DMPE) monolayer in the liquid condensed/liquid expanded (LC/LE) coexistence phase. Texas Red–DPPE was chosen because it partitions into the liquid expanded phase, leading to high contrast between the LE and LC phases using fluorescence microscopy.

In single-particle tracking, fluorescent polystyrene beads or highly scattering gold beads are optically visualized by video microscopy.⁹ The beads are either attached to membrane constituents to study their motion or directly incorporated into the membrane to act as passive diffusers. Since the random motion of individual tracers is observed directly, no assumptions about the nature of the diffusive behavior are required. However, to connect the random motion to the diffusion process a large, statistically significant number of position data are needed.¹⁵ This requirement is met by the use of a Langmuir monolayer as a membrane model. It provides the obser-

[†] University of Texas at Austin.

[‡] University of Leipzig.

(1) Levitz, P. In *Dynamics in Small Confining Systems IV*; Drake, J. M., Grest, G. S., Klafter, J., Kopelman, R., Eds.; Materials Research Society: Warrendale, PA, 1999; p 3.

(2) Pellenq, R. J.-M.; Rodts, Q.; Pasquier, V.; Delville, A.; Levitz, P. *Adsorption* **2000**, *6*, 241–249.

(3) Simson, R.; Yang, B.; Moore, S.; Doherty, P.; Walsh, F.; Jacobson, K. *Biophys. J.* **1998**, *74* (1), 297–308.

(4) Lodish, H.; Berk, A.; Zipursky, S. L.; Matsudaira, P.; Baltimore, D.; Darnell, J. *Molecular Cell Biology*, 4th ed.; W. H. Freeman: New York, 2000; Chapter 20.

(5) Toker, A. *Cell. Mol. Life Sci.* **2002**, *59*, 761–779.

(6) Pralle, A.; Keller, P.; Florin, E. L.; Simons, K.; Horber, J. K. H. *J. Cell Biol.* **2000**, *148*, 997–1007.

(7) Schutz, G. J.; Kada, G.; Pastushenko, V. P.; Schindler, H. *EMBO J.* **2000**, *19*, 892–901.

(8) Hess, S. T.; Huang, S.; Heikal, A. A.; Webb, W. W. *Biochemistry* **2002**, *41*, 697–705.

(9) Saxton, M. J.; Jacobson, K. *Annu. Rev. Biophys. Biomol. Struct.* **1997**, *26*, 373–399.

(10) Singer, S. J.; Nicolson, G. L. *Science* **1972**, *175*, 720–731.

(11) Schmid, S. L. *Annu. Rev. Biochem.* **1997**, *66*, 511–548.

(12) Parton, R. G.; Simons, K. *Science* **1995**, *269*, 1398–1399.

(13) Saxton, M. J. In *Membrane Permeability*; Academic Press: San Diego, 1999; Vol. 48, pp 229–282.

(14) Forstner, M. B.; Kas, J.; Martin, D. *Langmuir* **2001**, *17*, 567–570.

(15) Qian, H.; Sheetz, M. P.; Elson, E. L. *Biophys. J.* **1991**, *60*, 910–921.

vation area necessary for sufficiently long tracks of up to 50 000 steps.

Thus, a new experimental method has been developed that permits the simultaneous visualization of the random walks underlying diffusion processes as well as the anisotropic environment of the walker. The versatile method described will help elucidate the impact of inhomogeneous environments on two-dimensional diffusion and, in particular, the impact of the heterogeneous plasma membrane on lateral diffusion of membrane constituents.

Materials and Method

Vesicle Suspension and Bead Conjugation. The lipid monolayer is formed from a vesicle-containing subphase instead of being spread from an organic solvent. This has two major advantages: the preparation can be done in aqueous solution, allowing the use of particles and molecules incompatible with organic solvents; and free beads or excess molecules can be removed by centrifugation or dialysis.

DMPE (Avanti Lipids, Alabaster AL) was mixed with 0.5 mol % Texas Red labeled DPPE (Molecular Probes, Eugene, OR) with or without 0.05% biotin-DPPE (Molecular Probes), in a 2:1 chloroform to methanol solution. Any other monolayer component that is soluble in organic solvent can be added at this step. The mixture was spread on a Teflon plate (3 cm diameter) placed in a 50 mL glass beaker and dried under a vacuum for 6 h.

The buffer used for the vesicle preparation and the subphase was 100 mM potassium-free PBS buffer at pH 7.5, prepared with Millipore-H₂O (Millipore, Bedford, MA). PBS (5 mL) was added to the beaker containing the dried lipids. Additional water-soluble monolayer components can be added at this step, since they will be incorporated into the vesicle membranes during vesicle formation. The beaker was covered by Parafilm M (Fisher Scientific, Pittsburgh, PA) and heated at 55 °C for at least 8 h to allow the dried lipids to form vesicles in the aqueous buffer. Small vesicles form a monolayer faster because of a larger release in bending energy and faster diffusion to the surface. Thus the vesicles were ultrasonicated using a sonic dismembrator (Fisher Scientific, Suwanee, GA), which reduces the average diameter of the vesicles from several micrometers to a few hundred nanometers and facilitates a relatively rapid (2–4 h) formation of the monolayer.

NeutrAvidin-labeled, 0.2 μm diameter, yellow-green fluorescent polystyrene spheres (Molecular Probes) were used for a high contrast between beads and the monolayer. The beads were diluted with the potassium-free PBS buffer to 0.001% solids. Weakly aggregated multiple beads were dissociated by placing a tube with 10 mL of the solution in an ultrasonic cleaner (Ultrasonic Cleaner 1425, Branson, Danbury, CT) for 1 min. Immediately afterward, the solution was spun at 100 000g for 5 min to sediment remaining aggregates, and only the upper 5 mL of the supernatant was used. Subsequent visual control by counting under a fluorescent microscope (Zeiss Axiovert 100, 63 \times fluoro-plan objective, fluorescein filter set) showed less than 5% bead aggregates in the solution. The recently ultrasonicated vesicle suspension and the centrifuged bead solution were mixed in a 1:1 volume ratio, briefly vortexed, and conjugated at room temperature for 2 h. The vesicle-bead solution was diluted with 25 mL of the PBS buffer, vortexed, and centrifuged at 100 000g for 5 min to remove free beads, which remain in suspension. The pellet, containing the bead-labeled vesicles, was then resuspended in 2 mL of PBS. At this stage, over 90% of the remaining beads were incorporated in the vesicles as determined by counting under the fluorescence microscope. Although NeutrAvidin is a biotin binding protein, bead incorporation was independent of whether biotinylated lipids were included in the vesicles.

Langmuir Film Balance and Preparation of the Monolayer. To conduct diffusion measurements of single particles in monolayers at a fluid/air interface, external disturbances such as air movement and flows in the subphase must be minimized. For that purpose, a compact Langmuir film balance system was designed and built, and completely covered with an acrylic cover (AC) as shown in Figure 1a. The microscope objective (MO) has

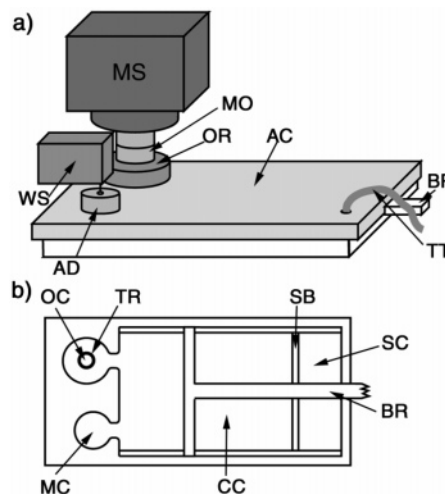


Figure 1. (a) Schematic side view of the compact Langmuir film balance enclosed by an acrylic cover (AC). Depicted are the microscope (MS) with objective (MO), the additional plastic ring around the objective (OR), the Wilhelmy system (WS) with the protective aluminum dome (AD), the end of the barrier/rod construct (BR) that connects to a linear actuator, and Teflon tubing that is connected to a syringe pump to regulate the filling level. (b) Top view of the trough showing the static barrier (SB) that divides the subphases of the spreading compartment (SC) and the main compression compartment (CC). Connected to the latter is the observation compartment (OC), containing an additional Teflon ring (TR) and the section in which the surface pressure is measured (MC).

a ring around it (OR), and the Wilhelmy system (WS) goes through a two-piece aluminum dome (AD) to reach the surface. Both the ring and the dome minimize openings in the cover and consequently reduce airflow in the trough.

The compression barrier is attached to a linear actuator outside the trough by a rod, manufactured from one piece of Teflon (BR) to fit under the cover. The phase state of the monolayer is controlled via compression or decompression by the movable barrier in the trough's main compartment (CC in Figure 1b).

To further suppress surface and subphase movement, the Langmuir trough itself is divided into four connected compartments (Figure 1b). In one of the two small, circular compartments (MC), the surface pressure of the monolayer is measured with the Wilhelmy system based on a PS4 microbalance (NIMA Technologies, U.K.). The monolayer is observed with the microscope in the other compartment, the observation compartment (OC), which also contains a Teflon ring (TR) that further suppresses subphase flow. All the measures taken reduce the drift of the monolayer, depending on the phase state, to values between 3 $\mu\text{m/s}$ (gaseous) and 1 $\mu\text{m/min}$ (crystalline) as determined by collective movement of particles fixed in the monolayer.

To keep the subphase of the observation compartment free of vesicles and thereby enhance the image quality, the main part of the Langmuir trough is divided by a stationary barrier (SB) blocking the exchange of the subphase. It is shaped such that the trough surface is continuous and the movable barrier can pass over it. The section SC is used to inject the vesicle suspension, and as the monolayer forms it spreads onto the surface of the vesicle-free compartments.

Video Microscopy, Image Analysis, and Tracking. The monolayer is observed using a fluorescent microscope in epillumination (Olympus BX-FLA, 50 \times 0.8 NA fluorescence/darkfield objective) equipped with a FITC/Texas Red dual fluorescence filter set (51006, Chroma, Brattleboro, VT). The images are acquired using a SIT camera (Dage-MTI VE-1000 SIT, Michigan City, IN; field of view, approximately 300 μm \times 200 μm) at 30 frames a second, digitized (National Instruments PCI 1407, Austin, TX), and stored on a hard drive array in real time. Generally about 10–50 particles are tracked at once for up to 30 min with an accuracy of 100 nm using the method described

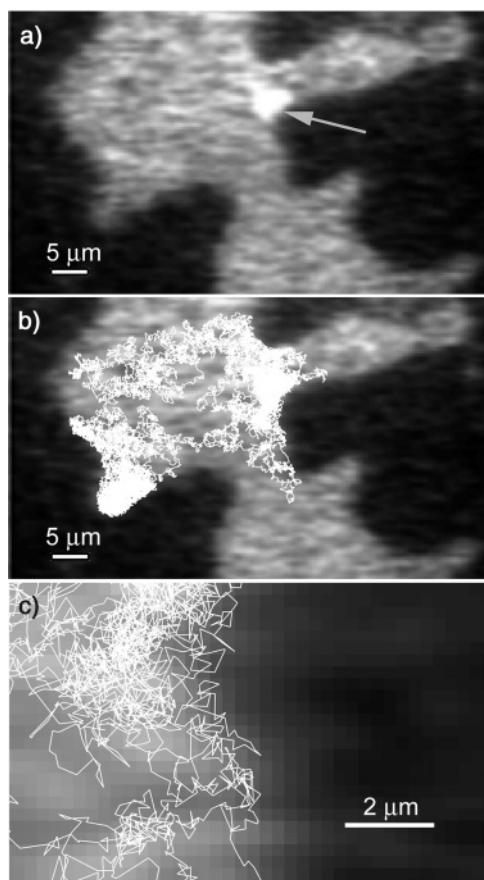


Figure 2. (a) A 200 nm fluorescent polystyrene bead (arrow) at the boundary of the liquid expanded (light gray) and the liquid condensed phase (dark gray) at a monolayer surface pressure of 16.0 ± 0.5 mN/m. (b) The overlay of the bead's random walk on the monolayer picture reveals no penetration into the liquid condensed domain. (c) The magnification of a portion of the random walk close to the domain boundary shows no visible interaction between the bead and the domain.

in Crocker et al.¹⁶ The position data are corrected for the spatial distortion introduced by the radial increasing pixel size and the rectangular pixel shape of the SIT camera before further analysis.

Immobile particles, incorporated in the LC phase, are used as reference points to obtain the remaining uniform drift motion of the monolayer. Subtracting the drift from the particles' movement leaves only their diffusive motion. From the corrected position data, the mean squared displacement (MSD) of the random walk is calculated as described in Gross et al.¹⁷ Deviations from normal two-dimensional diffusion ($\text{MSD}(t) = 4Dt$) are detected in the exponent of the time, t , since anomalous diffusion modes are characterized by a nonlinear growth of the MSD with time. In the case of normal diffusion, the diffusion coefficient D is determined from a linear fit to $\text{MSD}(t)$. In both cases, the effect of the inherent inaccuracy of the particle due to camera noise and its impact on the MSD was taken into account as described in Martin et al.¹⁸

Results and Discussion

Using this method, the fluorescent bead as well as the liquid condensed and the liquid expanded phase of the monolayer that correspond to the dark and bright features, respectively, are clearly visible (Figure 2a). The overlay of the reconstructed particle motion (Figure 2b) onto the

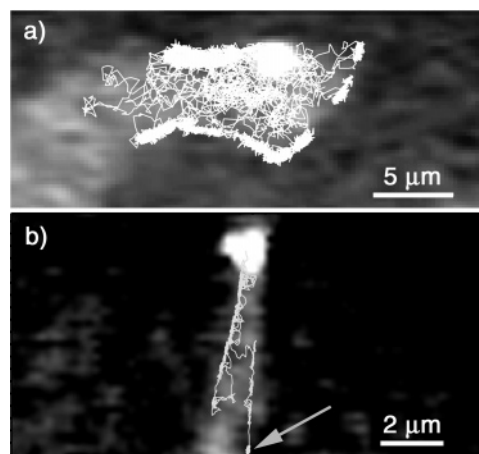


Figure 3. (a) Overlay of the random walk of a bead on the monolayer picture (surface pressure of 15.0 ± 0.5 mN/m). The bead follows the contour of the domain boundary for extended times, indicating an attractive interaction between bead and domain boundary. (b) The random walk of a bead (bright spot) between two nearby domains. The bead initially diffuses along the edges of the domains and becomes permanently attached to the right boundary at the position marked by the arrow. The surface pressure of the monolayer is 19.0 ± 0.5 mN/m.

monolayer structure shows that in the case of a DMPE monolayer, the liquid condensed phase cannot be penetrated by the diffusing particles. In addition, no difference between monolayers with and without biotin–DPPE is detected. This observation implies that the beads are embedded in the monolayer rather than bound to the biotinylated lipids. The track shown consists of 20 000 positions (~ 11 min) and permits therefore a reliable determination of the MSD scaling with time over three decades.¹⁵ The time scaling exponent of $\text{MSD}(t)$ is 0.95 ± 0.05 in accord with normal two-dimensional diffusion. The geometric confinement due to the LC domains will not affect the diffusion behavior within the first three decades, given the measured D and the size of the available LE phase.^{9,19} In this case, the diffusion coefficient D is determined from a linear fit to $\text{MSD}(t)$ and is 0.59 ± 0.01 $\mu\text{m}^2/\text{s}$.

The strength of our method is that this result can be connected to the underlying motion of the particle. It is immediately clear from the picture that the particle hits the domain. In addition, Figure 2c depicts a magnification of a subsection of the random motion and shows that the particle simply bounces off the domain boundary.

This suggests that the presence of the liquid condensed domains has only a confining impact on the diffusive motion of the particles. However, we were able to identify at least two more, qualitatively very different, types of bead–domain interaction, preventing such a conclusion at this point.

Figure 3a shows the motion of a different particle and its interaction with the domain boundary. In contrast to the reflection at the interface, the particle stays in the proximity of the boundary for up to 30 s where it undergoes diffusion only within a thin (~ 1 μm) band that runs parallel to the edge of the domain. These prolonged stays within this region are interrupted by excursions into the liquid expanded phase between domains. In addition, Figure 3b shows another particle that diffuses along the edges of two domains. However, at the end of the track, marked by the gray arrow, the particle becomes completely immobilized at the boundary for over 4000 steps (~ 100 s).

(16) Crocker, J. C.; Grier, D. G. *J. Colloid Interface Sci.* **1996**, *179*, 298–310.

(17) Gross, D. J.; Webb, W. W. In *Spectroscopic Membrane Probes*; Loew, L. M., Ed.; CRC Press: Boca Raton, FL, 1988; pp 19–45.

(18) Martin, D. S.; Forstner, M. B.; Kas, J. A. *Biophys. J.* **2002**, *83*, 2109–2117.

(19) Saxton, M. J. *Biophys. J.* **1993**, *64*, 1766–1780.

Our method makes it immediately clear that both of the changes in particle motion described above are linked to the presence of the liquid condensed domains.

Conclusion and Outlook

Although a DMPE monolayer in the LC/LE coexistence phase is a rather simple system compared to the cell's plasma membrane, it is important to understand these kinds of simplified systems, since they already exhibit complex behavior. In this case, the inhomogeneous environment has an observable impact on the tracks of diffusing particles. The key to optically visualize the interaction between the particles and the domains is the simultaneous detection of tracer motion and the imaging of the monolayer structure. This has been achieved by combining the Langmuir film balance technique, single-particle tracking, and dual fluorescence microscopy. Although this technique's potential use extends beyond the simple DMPE system, there are several interesting questions regarding the diffusion of the tracers in the

DMPE monolayer. For example, it is undetermined at this point if the interaction between particle and domain is of purely electrostatic character as the work of Nassoy et al.²⁰ might suggest or if other interactions have to be factored in.

Since the monolayer composition can be controlled, an extension to a multicomponent monolayer with complex domains and different phase states, like those in "lipid raft" mixtures, is straightforward, and the necessary modifications have already been mentioned in the methods section. Ultimately, this technique will help elucidate the connection between composition, structure, and phase state of two-dimensional disordered membranes and lateral mass transport through the membrane on the microscopic scale of single particles and its connection to macroscopic and thermodynamic processes.

LA034152U

(20) Nassoy, P.; Birch, W. R.; Andelman, D.; Rondelez, F. *Phys. Rev. Lett.* **1996**, *76*, 455–458.